
Faculty Work Comprehensive List

6-4-2021

Correlations Between the Strange Quark Condensate, Strange Quark Mass, and Kaon PCAC Relation

Derek Harnett

Jason N.E. Ho

Dordt University, jason.ho@dordt.edu

Tom G. Steele

Follow this and additional works at: https://digitalcollections.dordt.edu/faculty_work

 Part of the [Physics Commons](#)

Recommended Citation

Harnett, D., Ho, J. N., & Steele, T. G. (2021). Correlations Between the Strange Quark Condensate, Strange Quark Mass, and Kaon PCAC Relation. *Physical Review D*, 103 (11), 114005. <https://doi.org/10.1103/PhysRevD.103.114005>

This Article is brought to you for free and open access by Dordt Digital Collections. It has been accepted for inclusion in Faculty Work Comprehensive List by an authorized administrator of Dordt Digital Collections. For more information, please contact ingrid.mulder@dordt.edu.

Correlations Between the Strange Quark Condensate, Strange Quark Mass, and Kaon PCAC Relation

Abstract

Correlations between the strange quark mass, strange quark condensate ($\bar{s}s$), and the kaon partially conserved axial current (PCAC) relation are developed. The key dimensionless and renormalization-group invariant quantities in these correlations are the ratio of the strange to nonstrange quark mass $r_m = m_s/m_q$, the condensate ratio $r_c = \langle \bar{s}s \rangle / \langle \bar{q}q \rangle$, and the kaon PCAC deviation parameter $r_p = -m_s(\bar{s}s + \bar{q}q)/2f_2 K m_K^2$. The correlations define a self-consistent trajectory in the $\{r_m, r_c, r_p\}$ parameter space constraining strange quark parameters that can be used to assess the compatibility of different predictions of these parameters. Combining the constraint with Particle Data Group (PDG) values of r_m results in $\{r_c, r_p\}$ constraint trajectories that are used to assess the self-consistency of various theoretical determinations of $\{r_c, r_p\}$. The most precise determinations of r_c and r_p are shown to be mutually consistent with the constraint trajectories and provide improved bounds on r_p . In general, the constraint trajectories combined with r_c determinations tend to provide more accurate bounds on r_p than direct determinations. The $\{r_c, r_p\}$ correlations provide a natural identification of a self-consistent set of strange quark mass and strange quark condensate parameters.

Keywords

quantum chromodynamics, quark model, strong interaction, strange quark, chiral symmetry, flavor symmetries

Disciplines

Physics

Comments

Access on publisher's site:

<https://journals.aps.org/prd/abstract/10.1103/PhysRevD.103.114005>

Correlations between the strange quark condensate, strange quark mass, and kaon PCAC relation

D. Harnett^{1,*}, J. Ho^{2,†} and T. G. Steele^{3,‡}

¹*Department of Physics, University of the Fraser Valley, Abbotsford, British Columbia V2S 7M8, Canada*

²*Department of Physics, Dordt University, Sioux Center, Iowa 51250, USA*

³*Department of Physics and Engineering Physics, University of Saskatchewan, Saskatoon, Saskatchewan S7N 5E2, Canada*



(Received 22 April 2021; accepted 5 May 2021; published 4 June 2021)

Correlations between the strange quark mass, strange quark condensate $\langle \bar{s}s \rangle$, and the kaon partially conserved axial current (PCAC) relation are developed. The key dimensionless and renormalization-group invariant quantities in these correlations are the ratio of the strange to nonstrange quark mass $r_m = m_s/m_q$, the condensate ratio $r_c = \langle \bar{s}s \rangle / \langle \bar{q}q \rangle$, and the kaon PCAC deviation parameter $r_p = -m_s \langle \bar{s}s + \bar{q}q \rangle / 2f_K^2 m_K^2$. The correlations define a self-consistent trajectory in the $\{r_m, r_c, r_p\}$ parameter space constraining strange quark parameters that can be used to assess the compatibility of different predictions of these parameters. Combining the constraint with Particle Data Group (PDG) values of r_m results in $\{r_c, r_p\}$ constraint trajectories that are used to assess the self-consistency of various theoretical determinations of $\{r_c, r_p\}$. The most precise determinations of r_c and r_p are shown to be mutually consistent with the constraint trajectories and provide improved bounds on r_p . In general, the constraint trajectories combined with r_c determinations tend to provide more accurate bounds on r_p than direct determinations. The $\{r_c, r_p\}$ correlations provide a natural identification of a self-consistent set of strange quark mass and strange quark condensate parameters.

DOI: [10.1103/PhysRevD.103.114005](https://doi.org/10.1103/PhysRevD.103.114005)

QCD sum-rules techniques probe hadronic properties via QCD composite operators with appropriate quantum numbers and quark/gluonic valence content to serve as interpolating fields for hadronic states [1,2] (for reviews, see e.g., Refs. [3–5]). Correlation functions of these composite operators are calculated from QCD using the operator-product expansion and are then related to hadronic properties through dispersion relations, which are converted to a QCD sum rule through application of an appropriate transform. Important features of these correlation functions are the power-law corrections induced by QCD condensates (vacuum expectations values) that parametrize non-perturbative aspects of the QCD vacuum.

In QCD sum-rules analyses of hadronic systems containing strange quarks, the strange quark mass m_s , and the

strange quark condensate $\langle \bar{s}s \rangle$ are important parameters. Depending upon the system, the condensate may emerge as $\langle \bar{s}s \rangle$ or be accompanied with quark mass factors (e.g., $m_s \langle \bar{s}s \rangle$, $m_c \langle \bar{s}s \rangle$). However, $\langle \bar{s}s \rangle$ is also used within determinations of higher-dimension condensates, including the vacuum-saturation approximation for dimension-six quark condensates and the dimension-five mixed condensate [6,7]

$$\langle g \bar{s} \sigma_{\mu\nu} \lambda^a G_{\mu\nu}^a s \rangle = \langle g \bar{s} \sigma G s \rangle = ((0.8 \pm 0.1) \text{ GeV}^2) \langle \bar{s}s \rangle. \quad (1)$$

Because of these multiple roles in determining different QCD condensates, the strange quark condensate is an essential parameter in QCD sum rules and provides insight into $SU(3)$ flavor symmetry of the QCD vacuum.

QCD sum-rules studies of the strange quark condensate are based upon pseudoscalar and scalar correlation functions combined with low-energy theorems (see e.g., Refs. [8–10])

$$\Psi_5(q^2) = i \int d^4x \langle \Omega | T(J_5(x) J_5^\dagger(0)) | \Omega \rangle,$$

$$J_5(x) = i(m_u + m_s) \bar{s}(x) \gamma_5 u(x), \quad (2)$$

$$\Psi_5(0) = -(m_s + m_u) \langle \bar{s}s + \bar{q}q \rangle, \quad (3)$$

*derek.harnett@ufv.ca

†jason.ho@dordt.edu

‡tom.steele@usask.ca

Published by the American Physical Society under the terms of the [Creative Commons Attribution 4.0 International](https://creativecommons.org/licenses/by/4.0/) license. Further distribution of this work must maintain attribution to the author(s) and the published article's title, journal citation, and DOI. Funded by SCOAP³.

$$\Psi(q^2) = i \int d^4x \langle \Omega | T(J(x) J^\dagger(0) | \Omega \rangle, \quad (4)$$

$$J(x) = i(m_s - m_u) \bar{s}(x) u(x),$$

$$\Psi(0) = -(m_s - m_u) \langle \bar{s}s - \bar{q}q \rangle, \quad (5)$$

where $SU(2)$ isospin symmetry of the vacuum implies $\langle \bar{q}q \rangle = \langle \bar{u}u \rangle = \langle \bar{d}d \rangle$.

QCD sum-rules determinations of the low-energy constants $\Psi_5(0)$ and $\Psi(0)$ contain $\langle \bar{s}s \rangle$ dependence and thus provide a natural means to extract the strange quark condensate (see e.g., Refs. [8,9]). For example, the ratio $\Psi_5(0)/\Psi(0)$ can be used to reference the strange quark condensate to the nonstrange condensate through the renormalization-group (RG) invariant ratio and the RG invariant strange quark mass ratio $\xi = m_u/m_s = 0.024 \pm 0.006 \ll 1$ [11]

$$\frac{\Psi_5(0)}{\Psi(0)} = \left(\frac{1+\xi}{1-\xi} \right) \left(\frac{r_c+1}{r_c-1} \right) \approx \frac{r_c+1}{r_c-1}, \quad (6)$$

$$\frac{\langle \bar{s}s \rangle}{\langle \bar{q}q \rangle} = r_c, \quad \langle \bar{q}q \rangle = \langle \bar{u}u \rangle = \langle \bar{d}d \rangle. \quad (7)$$

Furthermore, as $\langle \bar{q}q \rangle < 0$, if $r_c < 1$ then $\Psi(0) < 0$, so the sign of the low-energy constant $\Psi(0)$ provides valuable information on qualitative aspects of $SU(3)$ flavor symmetry breaking by the vacuum.

There is a wide range of r_c theoretical determinations. QCD sum-rules analyses of light scalar and pseudoscalar meson correlation functions have been used to determine r_c [9,12–14], and a combined estimate from these results is $r_c = 0.57 \pm 0.12$ [4]. QCD sum rules for baryon mass splittings tend to yield larger values ranging from the earliest determinations $r_c = 0.8 \pm 0.1$ [15,16] to the updated values $r_c = 0.75 \pm 0.08$ [17] and $r_c = 0.74 \pm 0.03$ [18]. Because the QCD sum rules for heavy baryon mass splittings have better perturbative convergence compared to the light meson analyses, the most precise sum-rule value is $r_c = 0.74 \pm 0.03$ [18]. A more conservative sum-rule value obtained from an average of light meson and baryon systems is $r_c = 0.66 \pm 0.10$ [4]. The lattice QCD determination $r_c = 1.08 \pm 0.16$ [19] (multiple sources of uncertainty have been combined) is considerably larger than the sum-rules determinations. An analysis combining aspects of QCD sum-rules and lattice QCD results yields $r_c = 0.8 \pm 0.3$ [20]. The various theoretical determinations of r_c are shown in Fig. 1 and Table I.

The partially conserved axial current (PCAC) Gell-Mann-Oakes-Renner relation relates the RG invariant combination of the nonstrange quark condensate and mass parameter to pion properties [22]

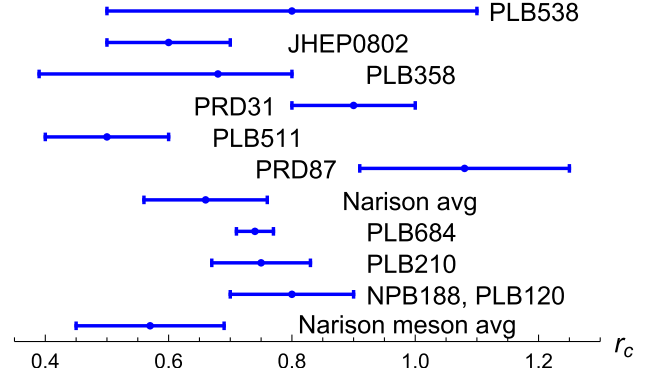


FIG. 1. Summary of r_c theoretical determinations. See Table I for key to references.

$$2m_q \langle \bar{q}q \rangle = -f_\pi^2 m_\pi^2, \quad m_q = \frac{m_u + m_d}{2}, \quad (8)$$

where in our conventions $f_\pi = 130/\sqrt{2}$ MeV [11]. Deviations from the pion PCAC relation are bounded by approximately 5% [10,19,20] and are thus a small numerical effect. The RG invariant quark mass ratio [11]

$$r_m = \frac{m_s}{m_q} = 27.3 \pm 0.7 \quad (9)$$

can then be combined with r_c to obtain the following strange quark condensate $m_s \langle \bar{s}s \rangle$ in terms of (8)

$$m_s \langle \bar{s}s \rangle = r_m r_c m_q \langle \bar{q}q \rangle. \quad (10)$$

A complementary approach to determinations of $m_s \langle \bar{s}s \rangle$ is through the deviation from the kaon PCAC relation as parametrized by r_p

$$-(m_s + m_u) \langle \bar{q}q + \bar{s}s \rangle \approx -m_s \langle \bar{q}q + \bar{s}s \rangle = r_p 2f_K^2 m_K^2, \quad (11)$$

where $r_p = 1$ corresponds to the kaon PCAC result (in conventions where $f_K = 156/\sqrt{2}$ MeV [11]) and (9) implies that neglecting m_u is a small numerical effect [see e.g., Eq. (6)]. The PCAC deviation parameter r_p can be determined in QCD sum rules by using the low-energy theorem for the pseudoscalar correlation function (3) (see e.g., Ref. [8]). A sum-rule evaluation of $\Psi_5(0)$ thus allows determination of r_p via Eqs. (11) and (3). Significant deviations from the kaon PCAC result have been found in this approach ranging from the earliest values $r_p = 0.63 \pm 0.08$ [8] and $r_p = 0.5 \pm 0.17$ [21], to later determinations from Laplace sum rules $r_p = 0.57 \pm 0.19$ [13],¹ QCD sum rules $r_p = 0.66_{-0.17}^{+0.23}$ [12], lattice QCD $r_p = 0.74 \pm 0.16$ [19], and combined approaches (merging Laplace sum

¹The result of [13] has been augmented with an estimated truncation error [4].

TABLE I. Summary of $\{r_c, r_p\}$ theoretical determinations shown in Figs. 1, 2, and 4. In some entries, multiple sources of uncertainty have been combined or ranges have been converted to an uncertainty. FESR denotes finite-energy sum-rules, LSR denotes Laplace sum rules, ChPT denotes chiral perturbation theory, QCDSR denotes QCD sum rules, AQCD denotes analytic continuation by duality, and LQCD denotes lattice QCD. The PLB511 entry includes a truncation uncertainty from Ref. [4].

| r_p | r_c | Reference | Methodology |
|------------------------|------------------------|--------------------------|---------------------------|
| 0.56 ± 0.16 | 0.5 ± 0.1 | [13] (PLB511) | LSR (four loops) |
| $0.66^{+0.23}_{-0.17}$ | $0.68^{+0.15}_{-0.29}$ | [12] (PLB358) | QCDSR |
| 0.57 ± 0.19 | 0.66 ± 0.1 | [4] (Narison avg) | QCDSR average |
| 0.66 ± 0.05 | 0.6 ± 0.1 | [14] (JHEP0802) | FESR five loop |
| 0.39 ± 0.22 | 0.8 ± 0.3 | [20] (PLB538) | ChPT, LSR, and LQCD input |
| 0.74 ± 0.16 | 1.08 ± 0.16 | [19] (PRD87) | LQCD |
| ... | 0.9 ± 0.1 | [9] (PRD31) | LSR |
| ... | 0.74 ± 0.03 | [18] (PLB684) | LSR heavy baryons |
| ... | 0.75 ± 0.08 | [17] (PLB210) | QCDSR heavy mesons |
| ... | 0.8 ± 0.1 | [15,16] (NPB188, PLB120) | QCDSR baryons |
| ... | 0.57 ± 0.12 | [4] (Narison meson avg) | QCDSR meson average |
| 0.5 ± 0.17 | ... | [21] (ZPC27) | LSR, AQCD |
| 0.63 ± 0.08 | ... | [8] (PLB104) | QCDSR |

rules, chiral perturbation theory, and lattice QCD input) $r_p = 0.39 \pm 0.22$ [20]. The most precise determination $r_p = 0.66 \pm 0.05$ emerges from finite-energy sum rules [14]. The various determinations of r_p are shown in Fig. 2.

The RG invariant combination of the strange quark mass and condensate emerging from the kaon PCAC relation (11) is

$$m_s \langle \bar{s}s \rangle = -r_p 2f_K^2 m_K^2 - r_m m_q \langle \bar{q}q \rangle. \quad (12)$$

The two expressions (10) and (12) for $m_s \langle \bar{s}s \rangle$ are thus self-consistent if the following constraint is satisfied:

$$r_c = \frac{r_p}{\sigma_m} - 1, \quad (13)$$

$$\sigma_m = r_m \left(\frac{f_\pi^2 m_\pi^2}{4f_K^2 m_K^2} \right), \quad (14)$$

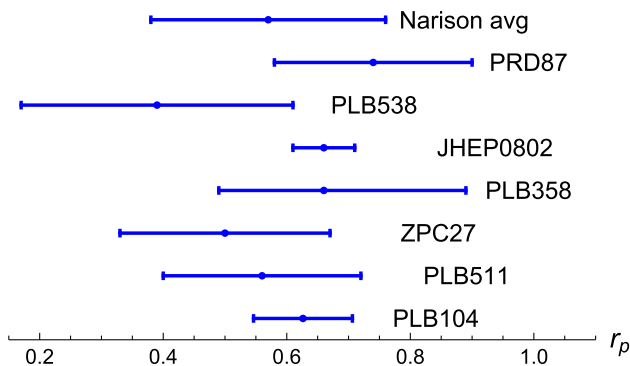


FIG. 2. Summary of r_p theoretical determinations. See Table I for key to references.

providing a correlation in the $\{r_m, r_c, r_p\}$ parameter space. The $\{r_c, r_p\}$ linear trajectories resulting from the PDG r_m range (9) are shown in Fig. 3. Determinations of r_c and r_p that lie along these trajectories will thus be self-consistent for the PDG range of the strange quark mass. The correlation trajectories provide a relatively more stringent constraint on r_p compared to r_c . For example, the conservative range $0.6 < r_c < 1.2$ leads to a relatively narrow range $0.57 < r_p < 0.86$ corresponding to a significant deviation from the kaon PCAC relation.

The most interesting analyses from the literature are those which simultaneously allow determination of both r_c and r_p because they map out a region in the $\{r_c, r_p\}$ parameter space that can be compared with the constraint trajectories. In Fig. 4, the simultaneous determinations of $\{r_c, r_p\}$ are compared with the linear constraint trajectories. The determinations from Refs. [4,12–14,19] show

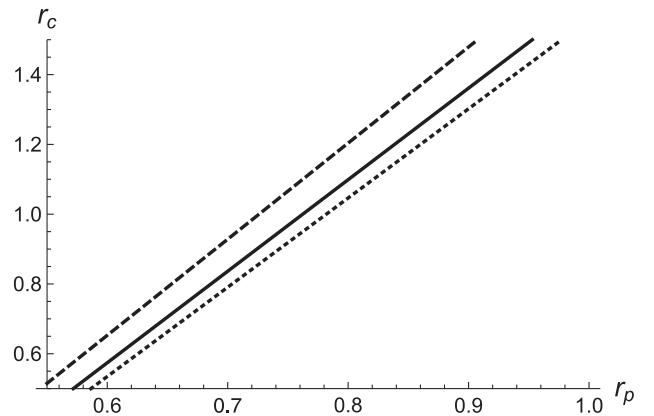


FIG. 3. Correlation (13) between r_p and r_c for PDG values [11] of r_m (solid black, dashed black, and dotted black lines respectively representing central, upper, and lower PDG values).

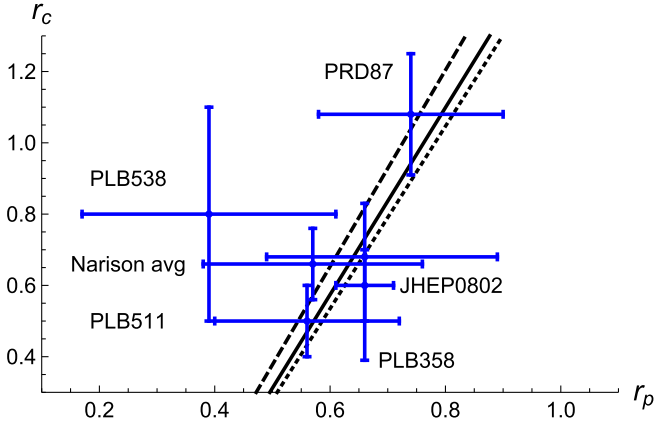


FIG. 4. Comparison of simultaneous $\{r_c, r_p\}$ determinations with the $\{r_p, r_c\}$ correlation trajectories (13) respectively representing central, upper, and lower PDG r_m values (solid black, dashed black, and dotted black lines). See Table I for key to references.

good agreement with the trajectories, but Ref. [20], which has the smallest determination of r_p , does not intersect the trajectories. However, Ref. [20] is somewhat different than the other simultaneous determinations in Fig. 4 because it combines different methodologies (the r_p determination in Ref. [20] involves chiral perturbation theory whereas r_c involves QCD sum rules).

As a final consideration, Fig. 5 assesses the most precise individual determinations $r_c = 0.74 \pm 0.03$ [18] and $r_p = 0.66 \pm 0.05$ [14] against the constraint trajectories. The two determinations delineate a compatible region of $\{r_c, r_p\}$ parameter space, and as discussed above, the r_c determination provides a tighter bound $0.62 < r_p < 0.69$ completely contained within the Ref. [14] determination.

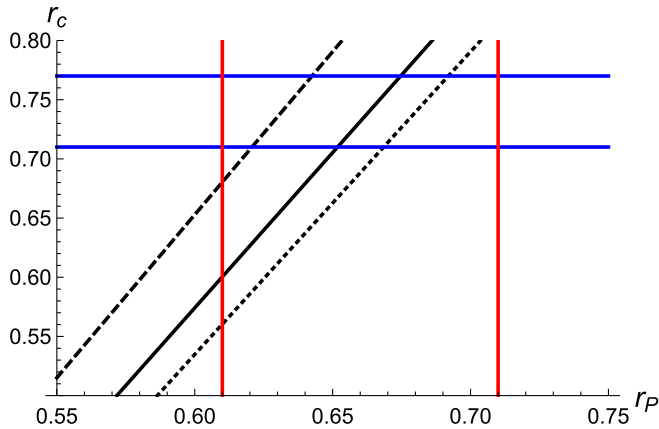


FIG. 5. Comparison of the Ref. [18] r_c bounds (blue lines) and Ref. [14] r_p bounds (red vertical lines) with the r_p, r_c correlation trajectories (13) respectively representing central, upper, and lower PDG r_m values (solid black, dashed black, and dotted black lines).

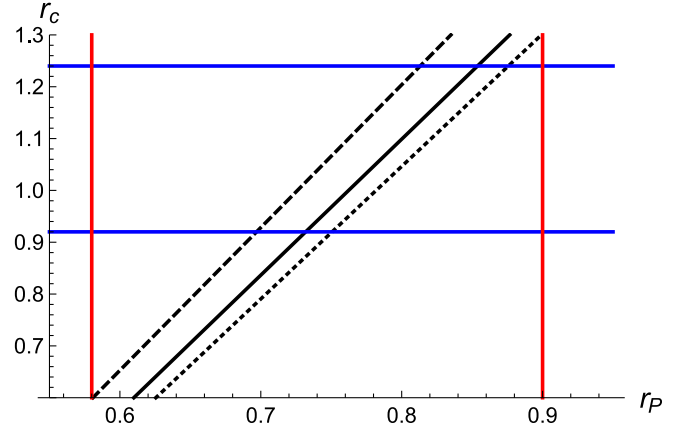


FIG. 6. Comparison of the Ref. [19] r_c bounds (blue lines) and r_p bounds (red vertical lines) with the r_p, r_c correlation trajectories (13) respectively representing central, upper, and lower PDG r_m values (solid black, dashed black, and dotted black lines).

A similar feature for the Ref. [19] lattice determinations is shown in Fig. 6; the constraint trajectories combined with the r_c determination again provide a tighter bound $0.69 < r_p < 0.88$ completely contained within the Ref. [19] determination. Thus the constraint trajectories combined with r_c determinations tend to provide more accurate bounds on r_p than direct determinations.

Based on a small set of input parameters, we can generate a collection of self-consistent numerical results for some QCD condensates containing strange quarks. The strange quark condensate $\langle \bar{s}s \rangle$ is often multiplied by a quark mass, *i.e.*, $M\langle \bar{s}s \rangle$, an RG invariant quantity. Using $r_c = 0.74 \pm 0.03$ and (8)–(10), we find

$$m_s \langle \bar{s}s \rangle = (-1.7 \times 10^{-3}) \text{ GeV}^4. \quad (15)$$

Then, using

$$m_c \langle \bar{s}s \rangle = \left(\frac{m_c}{m_s} \right) m_s \langle \bar{s}s \rangle, \quad (16)$$

$$m_b \langle \bar{s}s \rangle = \left(\frac{m_b}{m_s} \right) m_s \langle \bar{s}s \rangle \quad (17)$$

with quark mass ratios [11]

$$\frac{m_c}{m_s} = 11.72 \pm 0.25, \quad (18)$$

$$\frac{m_b}{m_s} = 53.94 \pm 0.12, \quad (19)$$

we find

$$m_c \langle \bar{s}s \rangle = (-1.9 \times 10^{-2}) \text{ GeV}^4, \quad (20)$$

$$m_b \langle \bar{s}s \rangle = (-9.0 \times 10^{-2}) \text{ GeV}^4. \quad (21)$$

Uncertainties in (15), (20), and (21) are at most 5% and stem mainly from deviations from pion PCAC in (8). Like $\langle \bar{s}s \rangle$, the dimension-five mixed strange quark condensate (1) is often multiplied by a quark mass, i.e., $M \langle g \bar{s} \sigma G s \rangle$. Equations (1) and (15) give

$$m_s \langle g \bar{s} \sigma G s \rangle = (-1.3 \times 10^{-3}) \text{ GeV}^6. \quad (22)$$

Then, again using the quark mass ratios (18) and (19), we find

$$m_c \langle g \bar{s} \sigma G s \rangle = (-1.6 \times 10^{-2}) \text{ GeV}^6, \quad (23)$$

$$m_b \langle g \bar{s} \sigma G s \rangle = (-7.2 \times 10^{-2}) \text{ GeV}^6. \quad (24)$$

Uncertainties in (22)–(24) are roughly 18% and stem from deviations from pion PCAC (8) and from the ratio of the strange quark condensate to the dimension-five mixed strange quark condensate in (1). Dimension-six quark condensates are often multiplied by a factor of α_s . In addition, the vacuum saturation hypothesis is generally used to express dimension-six quark condensates as products of dimension-three quark condensates [1]. Using

$$\alpha_s \langle \bar{q}q \rangle^2 = 1.8 \times 10^{-4} \text{ GeV}^6 \quad (25)$$

from Ref. [2], we find with $r_c = 0.74$ that

$$\alpha_s \langle \bar{s}s \rangle \langle \bar{q}q \rangle = 1.3 \times 10^{-4} \text{ GeV}^6, \quad (26)$$

$$\alpha_s \langle \bar{s}s \rangle^2 = 9.9 \times 10^{-5} \text{ GeV}^6. \quad (27)$$

Deviations from vacuum saturation can be applied by multiplying the results (25)–(26) by a vacuum saturation parameter κ where $1 \leq \kappa \lesssim 4$ (e.g., [23,24]). Note that the result (25) is remarkably consistent with (8) and the PDG [11] values $m_q(2 \text{ GeV}) = 3.45 \text{ MeV}$ and $\alpha_s(2 \text{ GeV})$.

In summary, we have developed the constraint (13) relating the strange quark parameters $r_m = m_s/m_q$, $r_c = \langle \bar{s}s \rangle / \langle \bar{q}q \rangle$ and the kaon PCAC deviation parameter $r_p = -m_s \langle \bar{s}s + \bar{q}q \rangle / 2f_K^2 m_K^2$. Using r_m PDG [11] values, $\{r_c, r_p\}$ theoretical determinations (see Table I) are compared with the constraint trajectories (see Fig. 4). Theoretical predictions corresponding to the smallest value of r_p show poor agreement with the constraint trajectories. However, Fig. 5 demonstrates that the most precise values $r_c = 0.74 \pm 0.03$ [18] and $r_p = 0.66 \pm 0.05$ [14] are mutually consistent with the $\{r_c, r_p\}$ constraint trajectories and provide an improved determination $0.62 < r_p < 0.69$. The combination of $\{r_c, r_p\}$ constraint trajectories with r_c determinations to obtain improved r_p bounds is also observed in Fig. 6 for the lattice values [19]. Thus the $\{r_c, r_p\}$ constraint trajectories provide a valuable methodology for assessing self-consistency or improving accuracy of determinations of the condensate ratio $r_c = \langle \bar{s}s \rangle / \langle \bar{q}q \rangle$ and the kaon PCAC deviation parameter $r_p = -m_s \langle \bar{s}s + \bar{q}q \rangle / 2f_K^2 m_K^2$.

ACKNOWLEDGMENTS

The work is supported by the Natural Sciences and Engineering Research Council of Canada (NSERC).

-
- [1] M. A. Shifman, A. Vainshtein, and V. I. Zakharov, *Nucl. Phys.* **B147**, 385 (1979).
 - [2] M. A. Shifman, A. Vainshtein, and V. I. Zakharov, *Nucl. Phys.* **B147**, 448 (1979).
 - [3] L. J. Reinders, H. Rubinstein, and S. Yazaki, *Phys. Rep.* **127**, 1 (1985).
 - [4] S. Narison, *QCD as a Theory of Hadrons From Partons to Confinement* (Cambridge University Press, Cambridge, England, 2007), <https://doi.org/10.1017/CBO9780511535000>.
 - [5] P. Gubler and D. Satow, *Prog. Part. Nucl. Phys.* **106**, 1 (2019).
 - [6] M. Beneke and H. G. Dosch, *Phys. Lett. B* **284**, 116 (1992).
 - [7] V. Belyaev and B. Ioffe, *Sov. Phys. JETP* **56**, 493 (1982).
 - [8] S. Narison, *Phys. Lett.* **104B**, 485 (1981).
 - [9] C. A. Dominguez and M. Loewe, *Phys. Rev. D* **31**, 2930 (1985).
 - [10] C. A. Dominguez, *Quantum Chromodynamics Sum Rules* (Springer International Publishing, New York, 2018), <https://doi.org/10.1007/978-3-319-97722-5>.
 - [11] P. A. Zyla *et al.* (Particle Data Group), *Prog. Theor. Exp. Phys.* **(2020)**, 083C01.
 - [12] S. Narison, *Phys. Lett. B* **358**, 113 (1995).
 - [13] C. A. Dominguez, A. Ramlakan, and K. Schilcher, *Phys. Lett. B* **511**, 59 (2001).
 - [14] C. A. Dominguez, N. F. Nasrallah, and K. Schilcher, *J. High Energy Phys.* **02** (2008) 072.
 - [15] B. L. Ioffe, *Nucl. Phys.* **B188**, 317 (1981); **B191**, 591(E) (1981).
 - [16] L. J. Reinders, H. R. Rubinstein, and S. Yazaki, *Phys. Lett.* **120B**, 209 (1983); **122B**, 487(E) (1983).
 - [17] S. Narison, *Phys. Lett. B* **210**, 238 (1988).
 - [18] R. M. Albuquerque, S. Narison, and M. Nielsen, *Phys. Lett. B* **684**, 236 (2010).

- [19] C. McNeile, A. Bazavov, C. T. H. Davies, R. J. Dowdall, K. Hornbostel, G. P. Lepage, and H. D. Trotter, *Phys. Rev. D* **87**, 034503 (2013).
- [20] M. Jamin, *Phys. Lett. B* **538**, 71 (2002).
- [21] C. A. Dominguez, M. Kremer, N. A. Papadopoulos, and K. Schilcher, *Z. Phys. C* **27**, 481 (1985).
- [22] M. Gell-Mann, R. Oakes, and B. Renner, *Phys. Rev.* **175**, 2195 (1968).
- [23] S. Narison, *Phys. Lett. B* **361**, 121 (1995).
- [24] R. A. Bertlmann, C. A. Dominguez, M. Loewe, M. Perrottet, and E. de Rafael, *Z. Phys. C* **39**, 231 (1988).